京都薬科大学紀要　3: 224–236, 2022
doi: 10.34445/00000355

原著

Computational investigation of polymer gel composition doped with ^{33}S for epithermal neutron measurement for BNCT

Kenichi Tanaka[1*], Tsuyoshi Kajimoto[2], Yoshinori Sakurai[3], Shin-ichiro Hayashi[4], Hiroki Tanaka[3], Takushi Takata[3], Gerard Bengua[5], Satoru Endo[2]

[1]Department of Physics, Kyoto Pharmaceutical University

[2]Graduate School of Advanced Science and Engineering, Hiroshima University

[3]Institute for Integrated Radiation and Nuclear Science, Kyoto University

[4]Faculty of Health Sciences, Hiroshima International University

[5]Auckland City Hospital

The purpose of this article is to find a suitable nuclear reaction for enhancing a polymer gel detector sensitivity for the quality assurance of epithermal neutron distribution in BNCT. As a method, simulations with PHITS was employed. Consequently, $^{33}S(n,\alpha)^{30}Si$ is promising. Required ^{33}S concentration in the detector was estimated based on epithermal neutron contribution to the energy deposition and on the irradiation field property. A 10 wt% satisfies the necessary contributions of 10%, 5%, and 1% at detector depths up to 5, 20, and 50 mm, respectively, for the epithermal neutron mode at KUR.

Keywords: boron neutron capture therapy, epithermal neutron, quality assurance, beam component, gel

受付日：2022 年 6 月 10 日，受理日：2022 年 9 月 29 日

1. Introduction

One way to do quality assurance (QA) on the profile of an irradiation field for boron neutron capture therapy (BNCT) is to monitor the spatial fluence distributions of the beam components, i.e., thermal neutrons (–0.5 eV), epithermal neutrons (0.5 eV–10 keV), fast neutrons (10 keV–), and gamma rays. A QA regime that is easy to implement as a routine verification method is desirable[1)]. Gel detectors have been useful for QA as it is able to measure three-dimensional dose distribution in photons and heavy ion irradiations[2, 3)], and in BNCT[4)]. Tanaka et al. have also demonstrated that gel detectors can separately measure the relative fluence of the com-

* 連絡先：
Department of Physics, Kyoto Pharmaceutical University
5 Misasaginakauchi-cho, Yamashina-ku, Kyoto 607-8414, Japan

ponents of a BNCT neutron field[5]. It was found that the MAGAT-type polymer gel detector doped with ^{6}Li at concentrations of 0, 10 and 100 ppm are usable for thermal and fast neutrons, and gamma rays. However, the dopant nuclide, and its concentration, for measuring the epithermal neutron component is yet to be found. The present paper investigated the suitable nuclide and the required condition for it to enhance the sensitivity of the gel detector to epithermal neutrons.

2. Materials and methods

The ^{33}S(n,α)^{30}Si reaction was considered as an initial candidate based on the work of Porras[6] which showed a dose increase from the epithermal neutron component. In addition, the cross section library JENDL-4.0 was surveyed for the reactions with high cross section for epithermal neutrons[7]. Of particular interest were reactions that produced charged particles such as (n,p), (n,α), and (n,t) which result in charged particles depositing energy in the polymer gel detector.

For the reactions selected, the required concentration of the reactant nuclide in the gel detector was estimated from the energy deposition in the gel detector calculated by the Monte Carlo code PHITS ver. 2.82[8]; the details of which were described by Tanaka et al.[5] and the procedure is briefly shown here. The irradiation field modeled was the standard epithermal neutron irradiation mode, at a power of 5 MW, of the Heavy Water Neutron Irradiation Facility at the Kyoto University Research Reactor Institute (KUR-HWNIF)[9]. The geometry consisted of a cylindrical gel detector with a diameter of 200 mm and a thickness of 200 mm. A 10×10 cm^2 beam was set on the circular face of the gel detector, with their central axes being aligned. The gel detector was divided into regions with the thicknesses of 5 mm in order to investigate the depth profile of the energy deposition. The gel detector considered in this work was the polymer gel detector which is composed of "Methacrylic Acid, Aelatin And an oxygen scavenger, i.e., Tetrakis-hydroxymetyl-phosphonium chrolide (THPC), called MAGAT. Its composition was H: 10.5 wt%, C: 9.5 wt%, N: 1.4 wt%, O: 77.7 wt%, P: 0.4 wt%, Cl: 0.5 wt%.

The cross section of the ^{33}S(n,α)^{30}Si reaction, the initial candidate reaction in this study, were obtained from JENDL-4.0, however, the data did not have the 13.4 keV resonance, which may have a role in enhancing the sensitivity of the gel detector to epithermal neutrons. The cross section around the resonance was then extracted from the work of Wagemans et al.[10] and added to the JENDL-4.0 data at energies from 12.8 keV to 14.3 keV. The resulting cross section is shown in **Fig. 1**. The cross sections for the other reactions are described later.

The nuclide selected was assumed to be doped into the gel detector as a simple substance with 100% atomic composition, as an ideal case. For the radiation transport calculation in the gel detector, the concentration of the nuclide selected was set to 10 wt%, as an example. Using the calculated energy deposition for each particle type and the neutron energy group corresponding to this concentration, the nuclide concentration required to measure epithermal neutrons was roughly estimated based on the criteria described later. A key point in this estimation is how high the measured beam component should have the relative contribution to the total of the energy deposition at the measured position in the gel detector. In the experimental study using an imaging plate, the estimated distribution of the beam components were shown to have reasonable

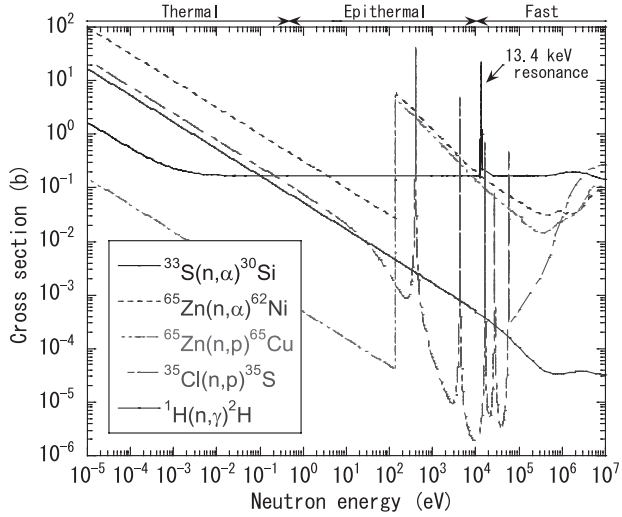

Fig. 1 Cross section used in the present study
The values of $^{33}S(n,\alpha)^{30}Si$ at 12.8–14.3 keV are from Wagemans et al. (1987) for a resonance at 13.4 keV, and the others are from JENDL-4.0.

distributions[11]. In this case, the beam components with the relative energy deposition contribution of 21% and 26% showed a reasonable result. Therefore, as an initial value, the necessary relative contribution to the energy deposition was assumed to be 26%. However, necessary relative contribution possibly changes according to the relative contribution of other beam components, and experimental uncertainties. Existing BNCT irradiation fields have different beam properties from each other and differ from a target value proposed in TECDOC-1223[12] by International Atomic Energy Agency (IAEA). Thus, the condition assumed in this study, i.e., the necessary relative contribution of epithermal neutrons to the energy deposition and the irradiation field property, is variable. Considering this, this study investigated the nuclide concentration needed to achieve the necessary energy deposition contribution and how such concentration depends on the necessary value of the relative energy deposition contribution and on assumed beam property.

3. Results and discussion

3.1 Selection of nuclide to sensitivity to epithermal neutron

From the survey of nuclear reactions, the maximum of the cross section at each energy region of thermal (–0.5 eV), epithermal (0.5 eV–10 keV), and fast (10 keV–) is shown in **Fig. 2**. The ratios of the cross section at the epithermal region in **Fig. 2** to those at other regions are shown in **Fig. 3**. The reactions $^{65}Zn(n,\alpha)^{62}Ni$, $^{65}Zn(n,p)^{65}Cu$, and $^{35}Cl(n,p)^{35}S$ were selected as the candidates to enhance the epithermal neutron sensitivity of the gel detector since their epithermal neutron cross sections in **Fig. 2** and cross section ratios in **Fig. 3** were comparable to those of $^{33}S(n,\alpha)^{30}Si$.

Among the candidates selected, ^{65}Zn with a half life of 244 days does not exist in nature. It should be produced by the neutron induction to ^{64}Zn (natural abundance: 49%). However, the reactions $^{65}Zn(n,\alpha)^{62}Ni$ and $^{65}Zn(n,p)^{65}Cu$ have a wide peak

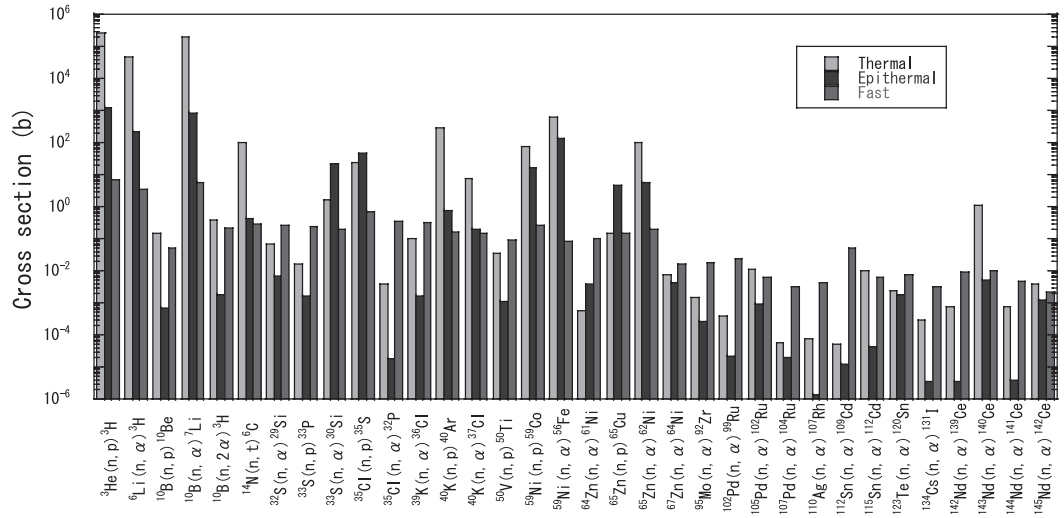

Fig. 2 Maximum of cross section in each energy region

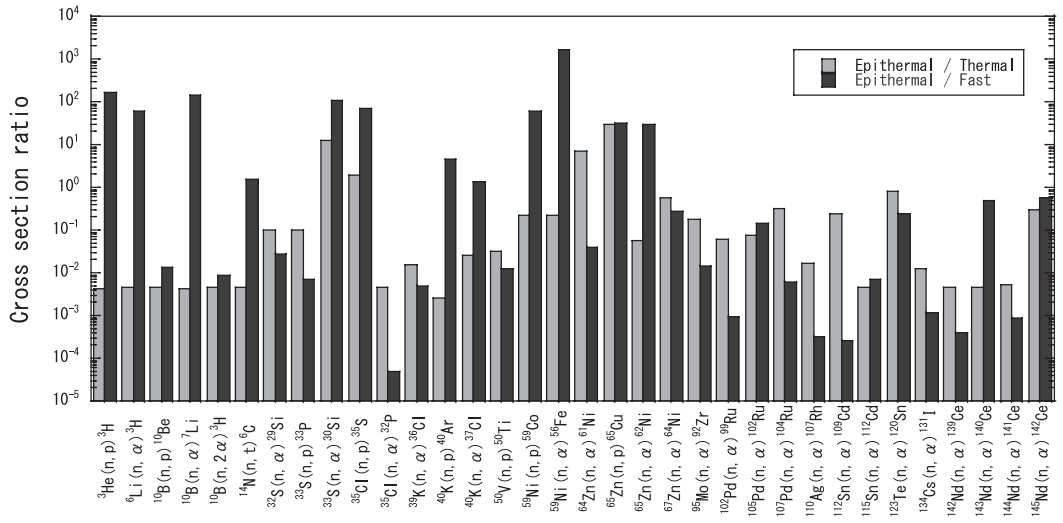

Fig. 3 Ratio of maximum cross section in epithermal region to that in other regions

over 100 eV and low cross section at thermal and fast regions from **Fig. 1**, and they are expected to efficiently enhance the influence of epithermal neutrons than other candidate nuclides. Therefore, apart from the convenience in practical use, this study investigated ^{65}Zn as a promising option as well as ^{33}S and ^{35}Cl.

The energy deposition shown in **Fig. 4** is for the gel detector with ^{33}S. The incident beam component in this case consists of all of four components, i.e., thermal, epithermal, fast neutrons and gamma rays. In **Fig. 4** (a), the majority of the energy deposition is via electrons. **Fig. 4** (b) shows the breakdown of the energy deposition via electrons. The component derived from neutron induction to the gel detector is dominant. This trend was also observed for ^{65}Zn and ^{35}Cl. The energy deposition via electrons in neutron induction is mainly from ^{1}H(n,γ)^{2}H reaction by

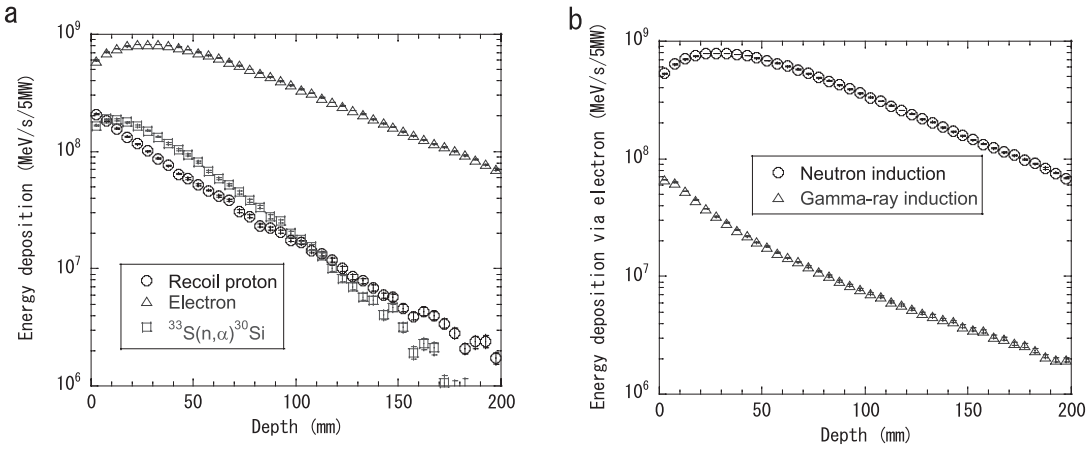

Fig. 4 Energy deposition in MAGAT with 10 wt% ^{33}S
(a) Dependence of energy deposition on its origin. (b) Breakdown of energy deposition via electron. The values correspond to the irradiation at KUR for 1 s at 5 MW of the power. The incident beam component in this case consists of all four components, i.e., thermal, epithermal, fast neutrons and gamma rays.

thermal neutrons; the dependence of its cross section on the neutron energy is also shown in **Fig. 1**. The relative contribution of each particle type or secondary particle from the reaction to the total energy deposition is shown in **Fig. 5** for the gel detectors with (a) ^{33}S, (b) ^{65}Zn, and (c) ^{35}Cl. At depths up to about 50 mm as an example, the relative contribution of the secondary particles from the $^{33}S(n,\alpha)^{30}Si$ reaction exceeds 10%.

The relative contribution of the neutron energy group to the energy deposition by secondary particles of each reaction is shown in **Figs. 6**. The epithermal contribution to $^{33}S(n,\alpha)^{30}Si$ is 10% or more at depths below 40 mm. The $^{33}S(n,\alpha)^{30}Si$ reaction has a resonance at 13.4 keV, which is close to the upper limit of the epithermal region at 10 keV. However, this upper limit is sometimes defined differently, e.g. 40 keV[12, 13]. In **Fig. 6** (a), the plots with the legend "Epithermal (0.5 eV–40 keV)" are for the epithermal energy range of 0.5 eV–40 keV. In this case, epithermal contribution increases by only several percents at depths up to about 50 mm. Therefore, except for the plots for Epithermal (0.5 eV–40 keV), this study uses 0.5 eV–10 keV as the epithermal range following IAEA definition, while the upper limit of the epithermal region is still an issue.

The relative contribution of each reaction by epithermal neutrons to the total energy deposition is shown in **Fig. 7**. The contributions of $^{33}S(n,\alpha)^{30}Si$ and $^{65}Zn(n,\alpha)^{62}Ni$ are below 10% respectively, and those of $^{65}Zn(n,p)^{65}Cu$ and $^{35}Cl(n,p)^{35}S$ are less than 1%.

The concentration of the doped nuclide in the gel detector required to achieve a 26% relative contribution of epithermal neutrons to the total energy deposition is shown in **Fig. 8**. The required concentration at depths up to 5 mm is 33 wt% for ^{33}S and 38 wt% for ^{65}Zn. The data at 2.5 mm corresponds to the depths from 0 to 5 mm since the gel detector was divided into the regions with the thicknesses of 5 mm in the calculations. The required concentration of ^{35}Cl is 350% or more, which is over 100 wt%. It suggests that it is impossible to realize a 26% epithermal contribution by including ^{35}Cl in the gel detector.

In **Fig. 6** (b), the epithermal contribution to the energy deposition by $^{33}S(n,\alpha)^{30}Si$ is 9% to 57% at

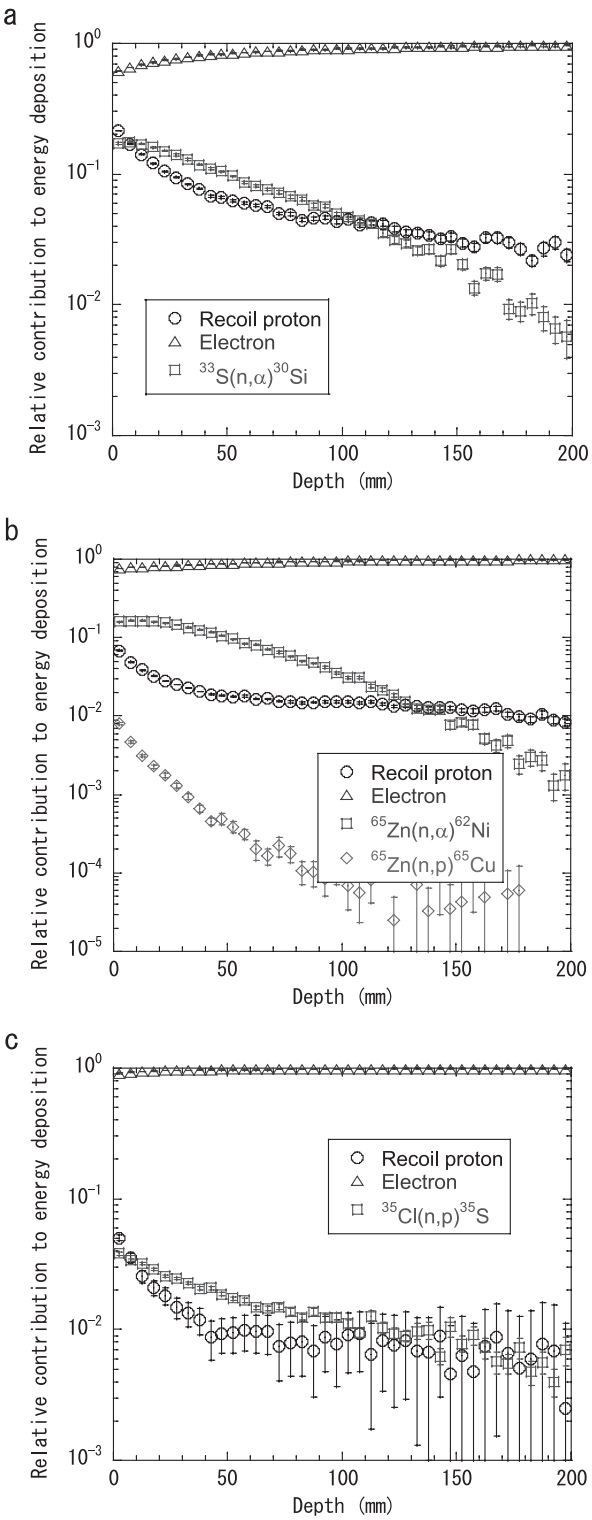

Fig. 5 Relative contribution of each particle type or reaction to total energy deposition at each depth in the gel detector doped with (a) ^{33}S, (b) ^{65}Zn, and (c) ^{35}Cl at 10 wt%

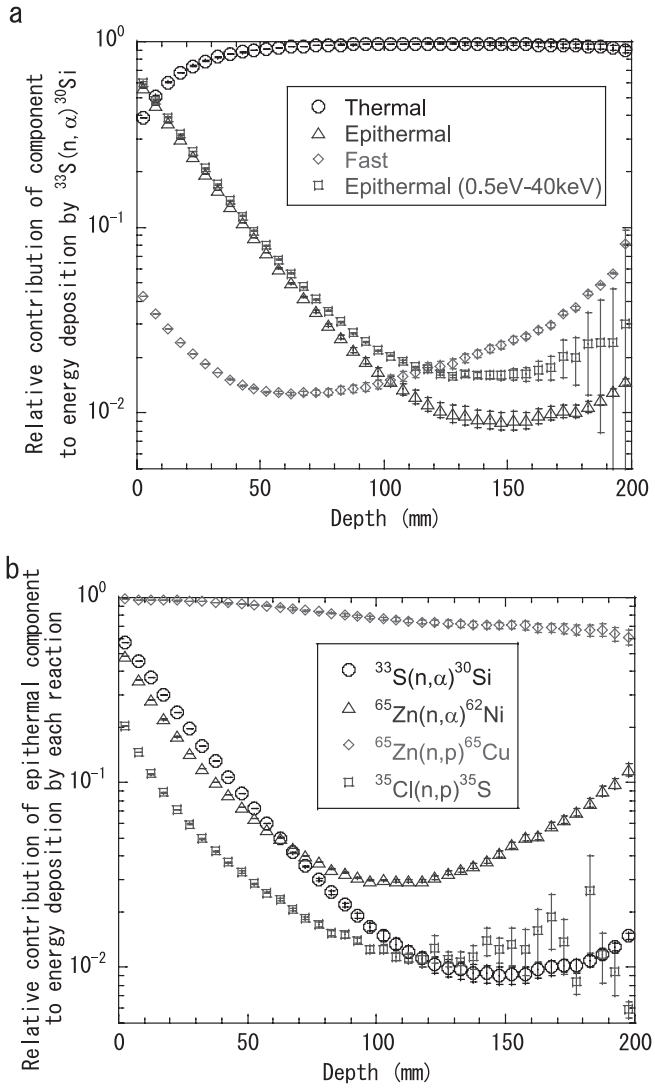

Fig. 6 Relative contribution of the (a) neutron component in each energy group to the energy deposition from $^{33}S(n,\alpha)^{30}Si$, (b) epithermal neutron component to the energy deposition by each reaction
The plots with the legend "Epithermal (0.5 eV–40 keV)" in Fig. 6 (a) are for the epithermal energy range of 0.5 eV–40 keV; the others are for 0.5 eV–10 keV.

depths up to 50 mm. On the other hand, a wide peak in the epithermal region and low cross section in the thermal and fast regions of $^{65}Zn(n,p)^{65}Cu$ cross section result in the epithermal contribution of about 100%, as shown in the same figure. However, in this case, the contribution of $^{65}Zn(n,p)^{65}Cu$ to the total energy deposition is lower than those of $^{33}S(n,\alpha)^{30}Si$ and $^{65}Zn(n,\alpha)^{62}Ni$ by one order or more in **Figs. 5** (a) and (b). Reflecting this, the relative contribution of $^{65}Zn(n,p)^{65}Cu$ by epithermal neutrons to the total energy deposition is about one order lower than those of $^{33}S(n,\alpha)^{30}Si$ and $^{65}Zn(n,\alpha)^{62}Ni$ by epithermal neutrons in **Fig. 7**. Also, for $^{33}S(n,\alpha)^{30}Si$ and $^{65}Zn(n,\alpha)^{62}Ni$, the energy deposition is dominated by the electron component in **Figs. 5** (a) and (b). This is derived from the relationship of the cross section

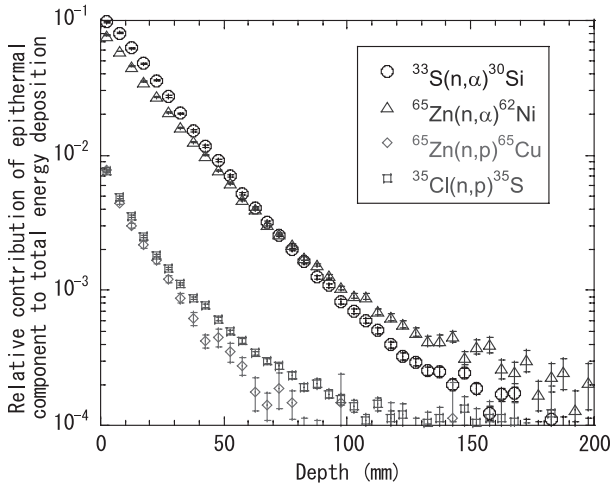

Fig. 7 Relative contribution of each reaction by epithermal neutrons to the total energy deposition

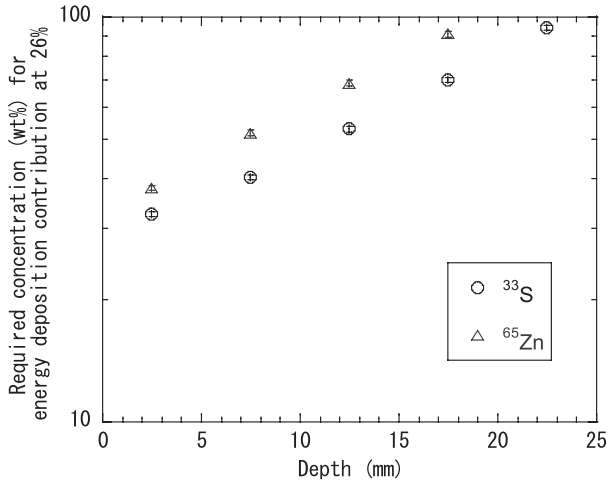

Fig. 8 Nuclide concentration required to realize 26% of relative contribution of epithermal neutrons to total energy deposition

between those reactions and $^{1}H(n,\gamma)^{2}H$ shown in **Fig. 1**.

It was found in our previous study that the gel detector with ^{6}Li at concentrations of 100 ppm or less are potentially usable in the quality assurance of the distributions of thermal and fast neutrons and gamma rays[5]. In order to reduce the required concentration of the doped nuclide for epithermal neutrons to the order of 100 ppm, the cross section with the energy dependence similar to those of $^{33}S(n,\alpha)^{30}Si$, $^{65}Zn(n,\alpha)^{62}Ni$, and $^{65}Zn(n,p)^{65}Cu$ should have values higher by three to four orders. Otherwise, the irradiation field will need three to four orders higher epithermal neutron intensity than the standard epithermal neutron irradiation mode of KUR-HWNIF. Although this study attempted to reduce the required concentration in the gel detector by using ^{65}Zn with its wide cross section peak in epithermal region, the required concentration resulted in the similar value for ^{33}S and ^{65}Zn in **Fig. 8**. We therefore

focus on ^{33}S in the succeeding discussion since it is stable and easier to handle.

3.2 Required ^{33}S concentration in gel detector

The standard epithermal neutron irradiation mode at KUR-HWNIF which was assumed in this study has different beam properties from what is proposed in IAEA-TECDOC-1223. It has a flux ratio of thermal to epithermal neutrons of 0.02, a fast neutron dose ratio to epithermal neutron fluence of 9.10×10^{-13} Gy cm^2, and a gamma-ray dose ratio to epithermal neutron fluence of 2.40×10^{-13} Gy cm^2; these are 0.4, 4.55 and 1.20 times higher than the IAEA proposal ratios, respectively. The required ^{33}S concentration to achieve the 26% epithermal contribution to the total energy deposition is shown in **Fig. 9** for the IAEA proposed irradiation field which was generated by scaling the calculated energy deposition for each beam component of the KUR epithermal mode. As mentioned earlier, the necessary epithermal contribution to the total energy deposition is variable. Thus, the concentrations for varied values of the necessary epithermal contribution are plotted in **Fig. 9** By setting the beam property to the one proposed by IAEA, the required concentration decreases by 20% to 30% for all the data points in **Fig. 9**. As the necessary epithermal contribution decreases, the required concentration decreases. On the other hand, for a constant ^{33}S concentration, the depth at which the necessary epithermal contribution is achieved increases. For example, for an epithermal contribution of 10%, the required concentration is 10 wt% up to 5 mm depth for KUR. When the epithermal contribution is 5%, the concentration of 5 wt% is required up to 5 mm depth, and 10 wt% up to 20 mm. In the case of a 1% epithermal contribution, the required concentration is 1 wt% to 5 mm, 5 wt% to 35 mm, and 10 wt% mm to 50 mm, which leads to the quality assurance of the distribution in deeper region.

3.3 Dependence on linear energy transfer

Many studies have investigated the dependence of gel signal intensity on linear energy transfer (LET).

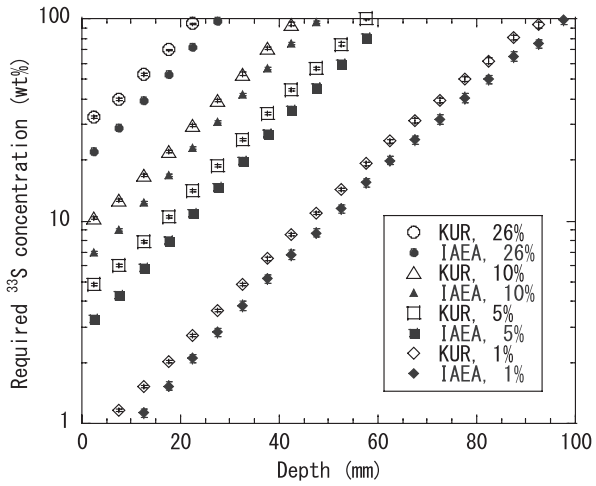

Fig. 9 ^{33}S concentration required for variable epithermal contribution to total energy deposition for standard epithermal neutron irradiation mode at KUR-HWNIF and irradiation field with target beam property by IAEA-TECDOC-1223
The percentage indicated in the legend specifies the necessary relative contribution of epithermal neutrons to the total of the energy deposition at the measured position in the gel detector.

Gustavsson et al.[14] showed the efficiency decreased for protons in the THP gel to one third compared to photons. Khajeali et al. reported that the efficiency in generating the signal for the N-isopropyl-acrylamide (NIPAM) gel for alpha particles is one third of that for photons[15]. Jirasek et al reported the decrease in efficiency of poly-acrylamide gel (PAG) for protons down to 20–39%[16]. The sensitivity dependence on the LET of the MAGAT gel with LiF has not been fully concluded. However, based on the results described in available literature, it would be reasonable to assume that sensitivities to protons, alpha particles, and other heavy charged particles are lower than that to electron by factor of 2 to 3. Thus, the required ^{33}S concentration will increase 2 to 3 times of the values described in sec. 3.2.

3.4 Distortion of component distribution by ^{33}S.

In practical QA, four gel detectors with different compositions will be prepared and irradiated separately. The dose absorbed in the gel detector will be read-out using an equipment for magnetic resonance imaging (MRI). The signal intensities are expressed by the equation:

$$\begin{pmatrix} S_1 \\ S_2 \\ S_3 \\ S_4 \end{pmatrix} = \begin{pmatrix} a_{11} & a_{12} & a_{13} & a_{14} \\ a_{21} & a_{22} & a_{23} & a_{24} \\ a_{31} & a_{32} & a_{33} & a_{34} \\ a_{41} & a_{42} & a_{43} & a_{44} \end{pmatrix} \begin{pmatrix} \Phi_1 \\ \Phi_2 \\ \Phi_3 \\ \Phi_4 \end{pmatrix} \quad (1),$$

where S_i denotes the intensity of the signal from the gel detector i, Φ_j denotes the fluence of the beam component j, and a_{ij} denotes the sensitivity of the ith gel to the jth component. The sensitivity is the signal intensity per unit amount of the beam fluence. The sensitivity is determined from actual measurement, simulation or a combination of both, in advance.

It is assumed that the relative relations between the fluences of the four components (Φ_1 through Φ_4) are identical for the four gel detectors, in estimating the beam component fluence using the equation (1). If this is not satisfied, then the solution will be different. In actual irradiation field, it is not possible that the relation is strictly the same among the gels. The influence of these differences should be included in the analysis, e.g., as a source of the uncertainty. In this sense, the fluence relation between the components should be as close as possible among the gel detectors.

Tanaka et al. showed that the intensity ratio of thermal and fast neutrons and gamma rays differed by tens of percent between the gel detectors for those beam components made of MAGAT doped with 0, 10, and 100 ppm of ^{6}Li[5]. In the present study, the beam component distributions were almost constant among the ^{33}S concentrations of 1 wt% or less, and differed slightly at 10 wt%. The difference of the fluence rate ratio of beam components to epithermal neutron component from that for MAGAT without ^{33}S is shown in **Fig. 10**. By addition of 10 wt% of ^{33}S, the fluence ratios differed from MAGAT without ^{33}S by 20–30% up to depths of 50 mm.

For the QA of the component distribution, i.e., not measuring the correct distribution but detecting the difference from the reference irradiation, the fluence relation between the four components may not always be the same among the gel detectors. The difference of the fluence between the gel detectors can be corrected as follows: in the equation (1), when the fluence of the component 1, Φ_1, in the gel detector 1 is β times higher than those in the gels 2 through 4, the signal intensity of gel 1 is expressed as

$$S_1 = \beta a_{11}\Phi_1 + a_{12}\Phi_2 + a_{13}\Phi_3 + a_{14}\Phi_4 \quad (2).$$

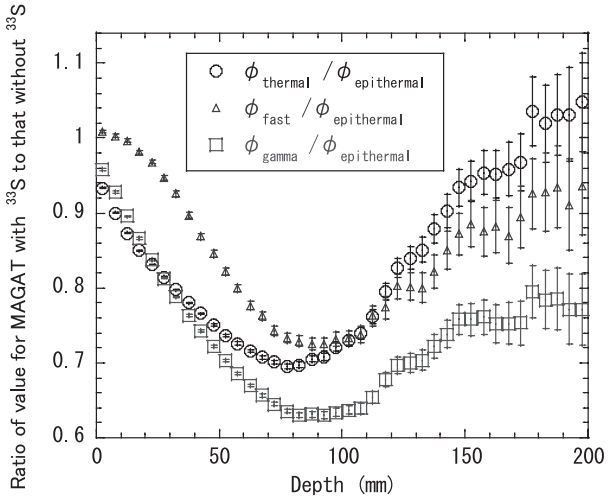

Fig. 10 Ratio of relationship between beam component fluence rates in MAGAT without ^{33}S to that in MAGAT without ^{33}S

The fluence of the beam components is assumed to be independent of gels 2 and 3, therefore their corresponding signal intensity is the same as those in equation (1)

$$S_2 = a_{21}\Phi_1 + a_{22}\Phi_2 + a_{23}\Phi_3 + a_{24}\Phi_4 \quad (3),$$

$$S_3 = a_{31}\Phi_1 + a_{32}\Phi_2 + a_{33}\Phi_3 + a_{34}\Phi_4 \quad (4),$$

$$S_4 = a_{41}\Phi_1 + a_{42}\Phi_2 + a_{43}\Phi_3 + a_{44}\Phi_4 \quad (5).$$

To correct for the change in the fluence Φ_1 in the gel 1, the sensitivity a_{11} in equation (2) should be replaced with a_{11}/β. Then, equation (2) now becomes the same as equation (1)

$$\begin{aligned} S_1 &= \beta(a_{11}/\beta)\Phi_1 + a_{12}\Phi_2 + a_{13}\Phi_3 + a_{14}\Phi_4 \\ &= a_{11}\Phi_1 + a_{12}\Phi_2 + a_{13}\Phi_3 + a_{14}\Phi_4 \end{aligned} \quad (6).$$

By estimating in advance the change in the fluence, β, by simulation calculation or experiment, the difference in the fluence between the gels can be compensated. Nevertheless, this process may be a source of the uncertainty. Ideally, the difference of the fluence should be as small as possible. This consideration does not prohibit the use of higher concentrations, but it is desirable to reduce the ^{33}S concentration in the gel detector to reduce the uncertainty due to fluence difference among the gels used. From this viewpoint, the usage of ^{33}S concentrations up to 10 wt% will be practical.

4. Conclusion

Potentially usable nuclide to enhance the sensitivity of the MAGAT-type polymer gel detector was investigated as a fundamental study of a method for the quality assurance of the spatial distribution of epithermal neutron fluence. The candidate of the nuclide was selected from the survey of the JENDL-4.0 cross section library so that the nuclide would have the reaction producing charged particles such as (n,p) and (n,α), with high cross section for epithermal neutrons. The usability of the selected nuclides was investigated by calculating the energy deposition to the gel detector doped with the nuclide at the concentration of 10 wt%, as an example, using the PHITS code. For the standard epithermal neutron irradiation mode at KUR-HWNIF, the contri-

bution of the epithermal neutron component to the energy deposition via secondary particles of the $^{33}S(n,\alpha)^{30}Si$ reaction to the gel detector doped with ^{33}S at 10 wt% is 9–57% up to about 50 mm depth in the gel detector. For the $^{65}Zn(n,p)^{65}Cu$ reaction, which was also selected through the survey, the epithermal contribution to the energy deposition by its reaction is about 100%. Accordingly, the required concentration of ^{65}Zn doped in the gel detector was expected to be lower than that of ^{33}S. However, as a result, the epithermal contribution to the total of the energy deposition was found to be 1% to 10% for both the nuclides at depths to 50 mm due to low cross section of those reactions. Consequently, from the viewpoint of the convenience in handling, ^{33}S was finally selected.

The ^{33}S concentration required was estimated with respect to its dependence on the necessary relative contribution of the epithermal neutron component to the total energy deposition to the gel detector. It was found that such concentration exists. For example, the concentration required for the epithermal neutron mode at KUR-HWNIF is 33 wt% for the necessary relative contribution of 26%, for which a reasonable distribution of the beam component was previously obtained using the imaging plate, at gel detector depths to 5 mm. The depth of the region where the necessary epithermal contribution is achieved increases as the necessary epithermal contribution decreases. For example, at ^{33}S concentration of 10 wt% for the epithermal neutron mode at KUR-HWNIF, the depth increases as 5 mm, 20 mm, and 50 mm for decreasing necessary contribution as 10%, 5%, and 1%, respectively. When the IAEA proposed irradiation field is used, the required concentration was reduced by 20% to 30% of what was required for the epithermal neutron mode at KUR-HWNIF. In this case, corresponding depths are 10 mm, 25 mm, and 55 mm, respectively. Considering the LET dependence of the gel sensitivity, the depth whether the epithermal contribution of 5% is achieved is 5 mm for IAEA irradiation field, and 25 mm and 30 mm for epithermal contribution of 1% for KUR-HWNIF and IAEA field, respectively.

In order to use the gel detector with nuclide to enhance the sensitivity of the gel detector at the order of 100 ppm, like ^{6}Li for separating thermal and fast neutrons and gamma rays, the nuclide should have the cross section that is three to four orders higher than $^{33}S(n,\alpha)^{30}Si$, $^{65}Zn(n,\alpha)^{62}Ni$, and $^{65}Zn(n,p)^{65}Cu$. However, it would not be easy to find such a reaction. In addition, it would not be practical to expect an irradiation field with epithermal neutron intensity higher by several orders than that of the epithermal neutron mode at KUR-HWNIF. Therefore, the key parameters that determine the feasibility of a quality assurance for epithermal neutron distribution are: (1) how high concentration of the nuclide can be realized in the gel detector and (2) how low epithermal neutron contribution to the energy deposition in the gel detector is acceptable. This study has demonstrated the investigation of whether one can use the selected nuclide and achievable parameters for it, including the further consideration of practical conditions such as the chemical form and atomic abundance of the nuclide.

【Acknowledgement】

This work was supported by JSPS KAKENHI Grant Numbers JP26293281 and JP20K08050. The authors express their sincere appreciation to Mr. Yuto Murakami in Hiroshima University and the Innovation Plaza in Hiroshima University (Especially to Mr. Seisuke Noguchi), Japan for their support in the investigations.

【Ethics approval and consent to participate】

There is nothing to declare.

【Conflict of Interest】

The authors declare no conflict of interest

【Reference】

1) Long Huang, Toufik Djemil, Tingliang Zhuang, Martin Andrews, Samuel Chao, John Suh, Ping Xia. Treatment plan quality and delivery accuracy assessments on 3 IMRT delivery methods of stereotactic body radiotherapy for spine tumors. *Med. Dosim.* **2018**, 44, 11–14.
2) Clive Baldock, Yves De Deene, Sude Doran, George Ibbott, Asam Jirasek, Moder Lepage, Krive McAuley, Michael Oldham, Luis Schreiner. Polymer gel dosimetry. Phys. *Med. Biol.* **2010**, 55, R1–R63.
3) Yves De Deene, Jasek Vandecasteele. On the reliability of 3D gel dosimetry. *J. Phys. Confr. Ser.* **2013**, 444, 012015.
4) Azim Khajeali, Ali Reza FaraJollahi, Roghayeh Khodadadi, Yaser Kasesaz, Assef Khalili. Role of gel dosimeters in boron neutron capture therapy. *Appl. Rad. Isot.* **2015**, 105, 72–81.
5) Kenichi Tanaka, Tsuyoshi Kajimoto, Aruma Mitsuyasu, Yuto Ito, Shin-ichiro Hayashi, Yoshinori Sakurai, Hiroki Tanaka, Takushi Takata, Gerard Bengua, Satoru Endo. Measurement of spatial fluence distribution of neutrons and gamma rays using MAGAT-type gel detector doped with LiCl for BNCT at Kyoto University Reactor. *J. Phys. Confr. Ser.* **2022**, 2167, 012006.
6) Ignacio Porras. Sulfur-33 nanoparticles: A Monte Carlo study of their potential as neutron captures for enhancing boron neutron capture therapy of cancers. *Appl. Rad. Isot.* **2011**, 69, 1838–1841.
7) Keiichi Shibata, Osamu Iwamoto, Tsuneo Nakagawa, Nobuyuki Iwamoto, Akira Ichihara, Satoshi Kunieda, Satoshi Chiba, Kazuyoshi Furutaka, Naohiko Otuka, Takaaki Ohasawa, Toru Murata, Hiroyuki Matsunobu, Atsushi Zukeran, So Kamada, Jun-ichi Katakura. JENDL-4.0; A new library for nuclear science and engineering. *J. Nucl. Sci. Tech.* **2011**, 48, 1–30.
8) Tatsuhiko Sato, Koji Niita, Norhihiro Matsuda, Shintaro Hashimoto, Yosuke Iwamoto, Shunsaku Noda, S., Tatsuhiko Ogawa, Hiroshi Iwase, HIroshi Nakashima, Tokio Fukahori, Keisuke Okumura, Tetsuya Kai, Satoshi Chiba, Takuya Furuta, Lembit Sihver. Particle and Heavy Ion Transport Code System PHITS, Version 2.52. *J. Nucl., Sci. Technol.* **2013**, 50, 913–923.
9) Yoshinori Sakurai, Tooru Kobayashi. Characteristics of the KUR Heavy Water Neutron Irradiation Facility as a neutron irradiation field with variable energy spectra. *Nucl. Instr. Meth.* **2000**, A453, 569–596.
10) Chris Wagemans, Huder Weigmann, Roy Barthelemy. Measurement and resonance analysis of the $^{33}S(n,\alpha)$ cross section. *Nucl. Phys.* **1987**, A469, 497–506.
11) Kenichi Tanaka, Yoshinori Sakurai, Hiroki Tanaka, Tsuyoshi Kajimoto, Takushi Takata, Jun Takada, Satoru Endo. Measurement of spatial distribution of neutrons and gamma rays for BNCT using multi imaging plate system. *Appl. Rad. Isot.* **2015**, 106, 125–128.
12) International Atomic Energy Agency, *Current status of neutron capture therapy. IAEA-TECDOC-1223*. **2001**, IAEA, Vienna, pp. 1–292.
13) Jacquelyn Yanch, Xu Zhou, Rosef Shefer, Roy Klinkowstein, Grif Brownell. Design of an accelerator-based epithermal neutron beam for boron neutron capture therapy. In: Barry Allen (Ed). *Progress in Neutron Capture Therapy for Cancer*. **1992**, Plenum Press, New York, pp. 107–112.
14) Helen Gustavsson, Sven Back, Joakim Medin, Erik Grusell, Lars Olsson. Linear energy transfer dependence of an normoxic polymer gel dosimeter investigated usin proton beam absorbed dose measurements. *Phys. Med. Biol.* **2004**, 49, 3847–3855.
15) Azim Khajeali, Ali Reza FaraJollahi, Yaser Kasesaz, Roghayeh Khodadadi, Assef Khalili, Alireza Naseri. Capability of NIPAM polymer gel in recording dose from the interaction of ^{10}B and thermal neutron in BNCT. *Appl. Rad. Isot.* **2015**, 105, 257–263.
16) Ali Jirasek, Christ Duzenli. Relative effectiveness of polyacrylamide gel dosimeters applied to proton beams: Fourier transform Raman observations and track structure calculations. *Med. Phys.* **2002**, 29, 569–577.